Principal Component Analysis As a Tool to Extract Sq Variation from the Geomagnetic Field Observations: Conditions of Applicability

Anna L. Morozova (annamorozovauc@gmail.com)
University of Coimbra Faculty of Sciences and Technology: Universidade de Coimbra Faculdade de Ciencias e Tecnologia https://orcid.org/0000-0002-8552-8052

Rania Rebbah
University of Coimbra: Universidade de Coimbra

Full paper

Keywords: Principal component analysis, Geomagnetic field, solar quiet variation (Sq), Coimbra Magnetic Observatory (COI)

Posted Date: January 18th, 2022

DOI: https://doi.org/10.21203/rs.3.rs-1148599/v1

Abstract

In this paper, we analyze the applicability of the principal component analysis (PCA) as a tool to extract the Sq variation of the geomagnetic field. We tested different geomagnetic field components and used data measured at different levels of the solar and geomagnetic activity and during different months. Geomagnetic field variations obtained with PCA were “classified” as Sq_{PCA} using two types of reference series: Sq_{IQD} series calculated using geomagnetically quiet days and simulations of the ionospheric field with models.

The results for the X and Y and Z components are essentially different.

The Sq variation is always filtered to the first PCA mode for the Y and Z components. Thus, PCA can automatically extract the Sq variation from the observations of the Y and Z components of the geomagnetic field.

For the X component, the automatic extraction of the Sq variation is not possible, and a complimentary analysis, like a comparison to a reference series, is always needed. We tested two types of reference series: the mean Sq_{IQD} and the outputs of the CM5 and DIFI3 models. Our results show that both the data-based and model-based reference series can be used but the DIFI3 model performs better. We also recommend estimating the similarity of the series not with the correlation analysis but using metrics that account for possible local stretching/compressing of the compared series, for example, the dynamic time warping (DTW) distance.

1 Introduction

There are three main types of geomagnetic field variations on the time scale from hours to several days: regular variations during a calendar or solar day (so-called “daily” or “solar” variations known as S-type variations), regular variations during a lunar month (L-variation) and irregular variations often associated with storms and substorms and called “disturbances” (Dst-variations), see Chapman and Bartels (1940). The S-type variations are divided into two main classes: the “daily (solar) quiet” variation, Sq, which is observed most clearly during the geomagnetically quiet days, and the “daily (solar) disturbed” variation, SD, (Chapman and Bartels, 1940; Yamazaki and Maute, 2017).

The Sq variation of the geomagnetic field results from an electrical current system in the ionospheric E dynamo region. This system consists of two vortices quasi-symmetric to the equator with the anti-clockwise (clockwise) electrical currents in the sunlit Northern (Southern) Hemisphere with foci located in the middle latitudes near 30-40º depending on the longitudinal sector and the hemisphere. Near the equator, they are connected to the equatorial electrojet, and in the high latitudes, they are affected by the current systems of the polar ionosphere. As the day progresses, the position of these vortices on the globe moves westward following the Sun. Thus, for any given location on the planet, the geometry of the system changes along the day returning to a similar condition after one day.

The character of the ground measured Sq variation of the geomagnetic field components X, Y and Z depends on the position of a geomagnetic observatory relative to the vortex. The change of the sign of Sq X takes place around the foci latitudes. The sign of Sq Y and Sq Z changes near the equator (see Chapman and Bartels, 1940; Amory-Mazaudier, 1994 and 2009; Anad et al., 2016; Yamazaki and Maute, 2017). The Sq X and Sq Z variations are symmetric around the local noon, while Sq Y is anti-symmetric. In the real ionosphere, the shape of the current vortex can be far from the ideal circle or oval: the vortex can, e.g., be tilted (resulting in a shift of the daily minimum of Sq X to the afternoon hours, see Amory-Mazaudier, 1994 and 2009; Anad et al., 2016), stretched or compressed. The shape of the vortex affects mostly the Sq X variation, whereas the shapes of the Sq Y and Sq Z variations are almost constant from day to day.

The standard method to obtain Sq from the ground observations of the geomagnetic field consists of the selection of days with the lowest level of geomagnetic field perturbations (so-called "quiet days"), typically, five days per calendar month, and averaging of the daily geomagnetic field variations for a certain component over selected days. These days can be defined using the data of an individual observatory (local quiet days) or using the data from the same set of observatories that are used to calculate the Kp index (international quiet days – IQD), see Chapman and Bartels (1940). Hereafter, the Sq variation obtained using IQD is named "Sq_{IQD}".

Another way to extract regular variations as Sq is to apply a decomposition method to the geomagnetic field data: e.g., the wavelet analysis (Maslova et al., 2010), the empirical mode decomposition (Piersanti et al., 2017) or the principal component analysis, PCA (Xu and Kamide, 2004; Chen et al., 2007; De Michelis et al., 2009, 2010). On the other hand, the shape and position of the vortex can be deduced from the observational data using the spherical harmonic analysis by calculating the equivalent electric field (Takeda, 1982; Haines and Torta, 1994) or it can be reconstructed as equivalent electric current vectors (horizontal component) from the observed horizontal geomagnetic field vector (Stening et al., 2005; Stening, 2008).

First attempts to use PCA (sometimes known as a method of the natural orthogonal component, NOC) to extract regular variations of the geomagnetic field were made in the 1970s-1990s (Golovkov et al., 1978, 1989; Rangarajan and Murty, 1980; Golovkov and Zvereva 1998, 2000) but were not actively supported by the geomagnetic community (Menvielle, 1981). Golovkov et al. (1978, 1989) and Golovkov and Zvereva (1998, 2000) showed that for the H component of the geomagnetic field and for the geomagnetically quiet time intervals, the Sq variation can be associated to the first (or first and third) principal components (PC) and the second PC can be identified as SD variation (Dst-like variation). For the geomagnetically active time intervals the first PC was identified as SD, and the second and third PCs were identified as Sq. Dependence of the order of a PC that can be identified as Sq or SD on the latitude was also shown. Both the existence of the daily variability of the Sq field and the need for studying it was also emphasized in the early works.

Later, Xu and Kamide (2004) and Chen et al. (2007) revived the interest of the geomagnetic community in PCA as a useful tool that allows not only to extract regular variations of the geomagnetic field, as Sq and SD but also to analyze seasonal and geographic variations of the phase and amplitude of the Sq and SD fields and the dependence of their intensity on the level of the solar and geomagnetic activity. Works of Wu et al. (2007), De Michelis et al., (2009, 2010), Bhardwaj et al. (2015, 2016) and others (see also review by Yamazaki and Maute, 2017), generally confirmed the applicability of PCA to the extraction of the regular geomagnetic field variations observed at different latitudes, and for the time intervals of different length and corresponding to different geomagnetic activity levels. However, the results obtained for different regions/time intervals were somewhat different.

In particular, it was found that for the H (X) component for the Asian sector (Xu and Kamide, 2004; Chen et al., 2007; Wu et al., 2007; Bhardwaj et al., 2015, 2016) the Sq variation is filtered to the first PC and the SD variation is filtered to the second PC. On the contrary, for the European sector (De Michelis et al., 2010) PC1 is associated with SD and PC2 is associated with Sq. This difference can be explained both by the different geographic positions of the stations whose data were used for PCA and by the different studied time intervals. Also, for the Y (D) and Z components for the European sector PC1 was identified as Sq and PC2 as SD.

To our knowledge, no systematic study of the applicability of PCA as a tool to extract Sq-type variations was performed yet and no possible explanation for the differences mentioned above was proposed. In this work, we present the results of such an analysis: we test PCA on different components of the geomagnetic field (X, Y and Z), for data obtained in different months and under different levels of solar and geomagnetic activity. We also tested different lengths of the input data sets. We use the geomagnetic field data obtained at a European mid-latitudinal geomagnetic observatory – Coimbra Magnetic Observatory (COI) in Portugal. The peculiarity of COI, and this can be also true for the L'Aquila observatory (De Michelis et al., 2010), is that it is located near the mean latitude of the focus of the Sq ionospheric current vortex. Thus, the shape of the Sq variations for the X component at COI can vary not only due to the intensity of the vortex but also due to the position of its focus: for some days COI is located to the north of the focus, for other days it is located to the south of the focus, and there are days when COI is located very near the focus latitude. These changes of the COI relative position result in different shapes of the Sq X variation. Finally, contrary to all previous studies, we analyzed the data not on the annual or decadal time scale but on the monthly time scale as described in section 2.1 and Morozova et al. (2021a, 2021b).

The paper is organized as follow: Section 1 presents the state of the art and briefly gives an overview of the paper; Section 2 contains the descriptions of the analyzed data sets; Section 3 describes the applied mathematical methods; the results of analyses of the applicability of PCA to extract Sq-type variation from data for different geomagnetic field components, limits of the PCA usage and ways to solve arising ambiguity are presented in Sections 4 (for the Y and Z components) and 5 (for the X component); Section 6 contains main conclusions on the usage of PCA as a tool to extract Sq-type variations from the geomagnetic field measurements.

2 Data

2.1 Geomagnetic field data

Geomagnetic measurements at the Coimbra Magnetic Observatory in Portugal (40º 13' N, 8º 25.3' W, 99 m a.s.l., IAGA code COI) have been started in 1866 (Morozova et al., 2014, 2021c). The last changes of the instruments took place at COI in 2006: new sets of the absolute instruments were installed providing good quality measurements of geomagnetic field components with 1 hour time resolution (Morozova et al., 2021c). Since that time to the present, there were no changes in the instruments or station location, and the data obtained between 2007 and the present time can be considered homogeneous (Morozova et al., 2021c). A detailed description of the COI instruments and metadata for the series of the geomagnetic field components can be found in Morozova et al. (2014, 2021a, c). The 1h data for all geomagnetic components can be downloaded from the World Data Centre for Geomagnetism using the Geomagnetism Data Portal at http://www.wdc.bgs.ac.uk/dataportal/ (station name: “Coimbra”, IAGA code: “COI”).

These data were used to obtain the Sq_{IQD} variation and the main PCA modes of the geomagnetic field variations analyzed in this paper. The analyzed dataset consists of 1h data on the variations of the X (northern), Y (eastern) and Z (vertical) components of the geomagnetic field measured at COI during 11 years from January 1, 2007, to December 31, 2017. This time interval covers (approximately) one solar cycle. The data for different components were analyzed separately. The data were analyzed on the time scale of one calendar month. The Sq_{IQD} variation and the PCA modes were calculated for each month both for the individual years, i.e., using only the data for January 2007, for January 2008, etc., separately, and for each month but all years together, i.e., using the data for January 2007 and January 2008, etc. together, hereafter “*all years*" series. As a result, for each of the three analyzed components, there were obtained 11*12 = 132 series for individual months and years, and 12 *“all years”* series. This dataset is described in detail in Morozova et al. (2021a) and is available at Morozova et al. (2021b). Standard errors (SE) for the Sq_{IQD} values were calculated for each month relative to the Sq_{IQD} *“all years”* series.

2.2 Solar and geomagnetic indices

To estimate the decadal and seasonal variations of the level of the solar and geomagnetic activities we used the following indices. The solar activity was represented by the daily means of the sunspot number series (R) and series of the F10.7 index reflecting variations of the solar UV flux. To describe variations of the geomagnetic activity level we used daily means of the Dst, Kp and ap, and AE indices. All the indices were obtained from the OMNI database at https://omniweb.gsfc.nasa.gov/form/dx1.html. The daily mean values of these indices were used to calculate both the monthly means and the IQD means (means calculated using only 5 IQD of a month) for each of the studied months. Corresponding plots can be found in the [Additional file 1, Figs. S1.1-S1.4].

3 Methods

3.1 Methods to obtain daily quiet variations of the geomagnetic field

In this work, we used two methods to obtain Sq variation of the geomagnetic field. One of these methods is the standard way to calculate Sq variation using IQDs. Another method is the application to the data of the principal component analysis. Both methods are described in detail in Morozova et al. (2021a) and the resulting series (both as data files and plots) are available at Morozova et al. (2021b). Here we give short descriptions of these methods.

3.1.1 Quiet days Sq

The standard approach to calculate Sq variation is to select days of a month with the lowest level of the geomagnetic activity. In this work, we used IQDs routinely provided by the GFZ German Research Centre for Geosciences at the Helmholtz Centre in Potsdam, Germany and available at https://www.gfz-potsdam.de/en/kp-index/ or ftp://ftp.gfz-potsdam.de/pub/home/obs/kp-ap/quietdst/.

The Sq variation for a certain month is calculated as the mean daily variation for five IQDs of a month. Before the averaging, a baseline was removed from the raw daily series of the X, Y and Z components. In this work, the baseline was defined as a mean calculated for the night hours: 00:30 UTC, 01:30 UTC, 02:30 UTC, 03:30 UTC and 23:30 UTC of each analyzed day (for Coimbra UTC = LT). Thus, the Sq variation values for the night hours are close to zero, and there is no significant difference between the night values of Sq at the beginning and the end of a day. Hereafter, these series are denoted as Sq_{IQD}.

3.1.2 Principal component analysis

Principal component analysis (PCA) allows the extraction of main modes of variability of an analyzed series. The full descriptions of the method can be found in Björnsson and Venegas (1997), Hannachi et al. (2007), Shlens (2009). PCs are orthogonal and conventionally non-dimensional. The amplitudes of a PC for each of the analyzed days are given by the corresponding empirical orthogonal functions (EOFs). The combination of a PC and the corresponding EOF is called a "mode". The "significance" of each of the extracted modes is estimated from the corresponding eigenvalues as variance fraction (VF). VF can be between 0 and 1 and multiplied by 100% shows the per cent of the total variability of the analyzed series related to a particular mode.

The PCA input matrices were constructed as follows. For the individual months and years, the input matrices have 24 rows (24 hourly values per day) and from 28 to 31 columns (a column for a day) depending on the analyzed month. All February matrices have the size 24 x 28. For the individual months but for the *“all years”* series the input matrices have sizes 24 x 308, 24 x 330 or 24 x 341, depending on a month. In this configuration of the input matrices, the principal components of PCA (PCs) correspond to daily variations of different types that can be matched up with Sq variation calculated using the standard approach. The amplitudes of PCs for an individual day are given by corresponding EOFs. The singular value decomposition (SVD) approach was used to solve matrix equations.

Only three first PCs were selected for further analysis. Overall, the first three PCA modes explain together up to 67-94% of the COI X variability, and up to 83-98% of the COI Y and COI Z series variability depending on a month and a year. Table 1 shows VFs associated with the first three PCA modes of the variations of the X, Y and Z components. During further analyses, those PCs that can be classified as Sq are denoted as Sq_{PCA}.

3.2 Simulation of the ionospheric part of the geomagnetic field

As reference series (see Section 5) for the ionospheric field of the X component of the geomagnetic field the ionospheric field generated by two geomagnetic field models, CM5 and DIFI3, were used. The CM5 and DIFI3 reference series were generated for the calendar day 15 of each of 12 months, from January to December. Since for both models the ionospheric field outputs for different years have the same shape but change only in the amplitude, the CM5 and DIFI3 reference series (Sq_{CM5} and Sq_{DIFI3}, respectively) were used in arbitrary units (a.u.). Detailed descriptions of the models can be found in Sabaka et al. (2002), and Chulliat et al. (2013, 2016) and Thébault et al. (2016), respectively, and short summaries are presented below.

3.2.1 CM5 model

CM5 is one of the versions of the so-called Comprehensive Models, developed to parametrize all the major near-Earth magnetic field sources: the core and the lithosphere fields, the M2 tidal component, the primary and induced magnetospheric fields, and the primary and induced ionospheric fields, all for different components of the magnetic field vector. They are developed by NASA/GSFC and the Danish Technical University. The details can be found in Sabaka et al., 2002. The model can be run online at https://ccmc.gsfc.nasa.gov/models/modelinfo.php?model=CM5.

CM5 was developed from the pre-Swarm satellite data (CHAMP, Oersted and SAC-CI) and observatory data from August 2000 to January 2013. Currently, a new version, CM6 (Sabaka et al., 2020), is available.

In our work, the CM5 model outputs for the primary and induced ionospheric field were summed to obtain a single reference series for the Sq-type variation.

3.2.2 DIFI3 model

The Dedicated Ionospheric Field Inversion (DIFI) model is a time-varying, spherical harmonic representation of the quiet-time Sq and the equatorial electrojet (EEJ) fields between ± 55° quasi-dipole latitudes. It is derived from a combination of Swarm satellite and magnetic observatory data: the 0501 L1b Swarm data and observatory data between December 1, 2013, and January 29, 2017. Time variations are represented by Fourier series with periods of 24h, 12h, 8h and 6h, modulated by annual and semi-annual periodicities. The spherical harmonic expansion goes to degree 60 and order 12 in geomagnetic dipole coordinates. Solar activity (represented by the F10.7 index) dependence is also

included in the model. Conductivity models of oceans and continents have been used to separate primary and induced magnetic fields (Chulliat et al., 2013, 2016; Thébault et al., 2016).

The DIFI model is developed by CIRES in collaboration with the Institut de Physique du Globe de Paris (IPGP) through Swarm's Satellite Constellation Application and Research Facility (SCARF), a project funded by the European Space Agency (ESA). DIFI is an official level 2 product of the Swarm mission. DIFI models and other Swarm level 2 products are also available at https://earth.esa.int/web/guest/swarm/data-access. The model can be run online at http://geomag.colorado.edu/difi-calculator.

3.3 Classification of PCs

In this work, the daily variations obtained by PCA (PC1, PC2 and PC3) were compared to the Sq_{IQD}, Sq_{CM5} and Sq_{DIFI3} variations and classified, when possible, as Sq_{PCA} using two classification metrics: (1) the absolute value of the Pearson correlation coefficient (r), and (2) a metric called the dynamic time warping (dtw). Short descriptions of these metrics are given in Sections 3.3.1 and 3.3.2, respectively.

We tested two approaches to the PCs' classification: allowing the combined classification (either one or a sum of two PCs can be classified as Sq_{PCA}) and not allowing the combined classification, i.e., single classification (only one PC per studied month is classified as Sq_{PCA}). The need for the combined classification can be justified by the possibility of PCA to decompose an Sq-type variation into several modes for months when the solar and geomagnetic activities were very low. In such a case an Sq-type variation can be decomposed by PCA into several modes that contain different fine features of Sq. The sums of PCs were calculated as weighted sums with weights being the monthly mean values of the corresponding EOFs.

For each set of PCs, the classification metrics were calculated between those PCs (their sums) and the corresponding reference series (Sq_{IQD}, Sq_{CM5} or Sq_{DIFI3}). Only PC or a sum of PCs with metrics that are above (below) a predefined threshold for r (dtw) are used for further classification, and PC or a sum of PCs with highest (lowest) values of r (dtw) was classified as Sq_{PCA}.

3.3.1 Correlation analysis

We used the standard Pearson correlation coefficient. Since in this work we used the SVD method to perform PCA, the PCs and EOFs are resolved accurately to a sign. This is because both 1*PC & 1*EOF, and -1*PC & -1*EOF are solutions for an input PCA matrix. There is no general way to solve the sign ambiguity. Keeping this in mind we used the absolute values of the correlation coefficients $|r|$. The threshold for the classification using the correlation analysis was set as $|r| \geq 0.45$.

The significance of the correlation coefficients was estimated using the Monte Carlo approach with artificial series constructed by the "phase randomization procedure" Ebisuzaki (1997). The obtained

statistical significance (*p value*) considers the probability of a random series to have the same or higher |*r*| as in the case of a tested pair of the original series.

3.3.2 Dynamic time warping

When using the correlation coefficient as a measure of similarities between two series one must remember that its value is affected mostly by the similarity of main features existing in the compared series. It may be not sensitive to small-scale features or non-systematic shifts of the local minima or maxima (systematic shifts of the local minima and maxima or a relative shift of a whole series can be accounted for by the lagged correlation analysis). Thus, we would need a metric that is sensitive to irregular deformation of series.

The dynamic time warping (DTW) is a popular metric for comparing time series that is insensitive to local compression and stretches allowing to optimally deforms one of the two input series onto another and calculate a certain measure for the “distance” (*dtw*) between the studied series (Giorgino, 2009). The smaller the “distance” the higher the similarity between the series, contrary to the correlation coefficient which is higher in the absolute value for the similar series. A description of the DTW algorithm can be found in Giorgino (2009, see also reference herein).

In short, when the similarity of two-time series is studied, one of the series is taken as a "reference" and another is locally stretched or compressed to make it resemble the "reference" as much as possible. The distance (*dtw* value) between the two series is computed after all stretching/compressing are finished by summing the distances of individual aligned elements. Several DTW algorithms have been proposed in the 1970s in the context of speech recognition (Giorgino, 2009).

The *dtw* parameter, contrary to *r*, is not defined on a certain absolute scale. To be able to compare the *r* and *dtw* values we had to (1) use standardised (zero mean and unity standard deviation) series to perform the DTW analysis and (2) to compare *r* and *dtw* sets obtained for the same pairs of series to see if there is any correspondence between the values of *r* and *dtw.* In our tests, it was found that this correspondence can be well fit by Eq. 1

$$dtw = \frac{A(1 - r)}{B + (1 - r)}$$

1

,

where A and B are fitting coefficients. An example of a *dtw* fit on *r* is shown in the [Additional file 2, Fig. S2.1] and [Additional file 2, Table S2.1] presents *dtw* values for certain *r* when PCs series are compared to different reference series (see Section 5).

The mean *dtw* threshold that is equivalent to $|r| \geq 0.45$ is $dtw \leq 0.58$ but for individual pairs of PCs vs a reference series, it varies from 0.57 to 0.62. As is shown in Section 5 the DTW analysis allows for better

estimation of the similarity of studied series than the correlation analysis, and the number of the classified series using this *dtw* threshold is higher than the number of the classified series using the correlation analysis with the $|r| \geq 0.45$ threshold.

4 Performance Of Pca As A Tool To Extract Sq For The Y And Z Components

The main goal of the work presented here is to analyze the ability of PCA to extract Sq-type variation from geomagnetic data and find constraints, if any, on the applicability of PCA for such purpose.

In general, such ability was already shown in previous works (see, e.g., Golovkov and Zvereva, 1998 and 2000; Xu and Kamide, 2004; Chen et al., 2007; De Michelis et al., 2010) and is valid on the following grounds. The main PCA modes represent the most prominent and the most regular variations existing in the analyzed data series. Since regular daily Sq-type variations are the most regular variations of the geomagnetic field, especially for the Y and Z components, it is expected for the Sq-type variations to be extracted as one of the first PCA modes.

Here we provide a systematic analysis of the PCA's performance on mid-latitudinal geomagnetic data for different geomagnetic field components, different seasons and under different levels of the solar and geomagnetic activity. We also tested if only one PC is always sufficient to represent an Sq-type variation or a combination of two PCs should be considered as well.

As the first step, we studied the PCA performance for the Y and Z components: for these components, the S-type variation is robust and dominant, and the results obtained for the X component are discussed in Section 5.

The Sq_{IQD} series of the Y and Z components have very stable and specific shapes (see, for example, the width of the Sq_{IQD} ±SE bands in Fig. 1): the Sq_{IQD} Z variation is symmetric around the local noon, while Sq_{IQD} Y is anti-symmetric. These shapes agree well with the shapes of the Sq variations for the Y and Z components expected at a mid-latitudinal geomagnetic station (see, e.g., Chapman and Bartels, 1940; Amory-Mazaudier, 1994 and 2009; Anad et al., 2016). Figure 1 shows examples of the first PCs together with Sq_{IQD} for the Y (top panel) and Z (bottom panel) components. The series for PC1s-PC3s and Sq_{IQD} for all months and all years can be found at Morozova et al. (2021b).

The comparison of PC1-PC3 obtained for the Y and Z components with corresponding Sq_{IQD} using the correlation analysis shows that all the PC1 series for both components can be reliably classified as Sq_{PCA}. Figure 2 shows tile plots with the classification of PC1s for Y and Z with numbers showing values of the correlation coefficients (all $|r| \geq 0.88$, all $p\ value < 0.01$). PC2s of the Y and Z series rarely have a significant correlation with Sq_{IQD} (only 1 case out of 144 for Y and Z, respectively, $|r| = 0.48$-0.55, $p\ value > 0.2$), and no PC3 has such correlations (corresponding plots can be found in [Additional file 3, Figs. S3.1-S3.4]. The use of the combined classification does not significantly improve the classification of PCs: the addition of other PCs to PC1 increases the *r* values insignificantly (please compare Fig. 2 and Figs. S3.1-

S3.2 with Figs. S3.3-S3.4 in [Additional file 3]). Therefore, the combined classification is not needed in the case of the Y and Z components.

Thus, for the Y and Z components for all analyzed months and all 11 years from 2007 to 2017, the PC1 series are defined as Sq_{PCA}. This means that Sq is the dominant variation for these components. This also means that for the Y and Z components the probability for Sq variation to be extracted as PC1 is 100%, and, therefore, PCA can be used as a reliable method to extract Sq variations from the Y and Z series when the use of IQD is not possible or not applicable for some reason (e.g., gaps in the analyzed series of the geomagnetic measurements or the overall high geomagnetic activity level of the studied months). Also, for the Y and Z components, the PCA performance does not depend on the season or the level of the solar/geomagnetic activity.

Using PCA we can estimate a part of the variability of the original Y and Z series associated with the Sq variation. As follows from Tab. 1, the mean variance fraction for PC1 for the Y and Z components is ~84%. There is a seasonal variation of VF associated with PC1: it is higher during the summer months and lower during winter. These seasonal variations of VF are not driven by the part of the geomagnetic activity, which is described by the Kp, ap or Dst indices: these indices have semi-annual cycles (see Fig. S1.3-S1.4 in [Additional file 1]). On the other hand, the AE index describing the geomagnetic activity related to the high-latitudinal magnetosphere and ionosphere has an annual cycle with a maximum in summer (see Figs. S1.3-S1.4). However, to our mind, the main reason for an increase of VF for the first PCA mode during summer is the overall increase of the insolation and the intensification of the Sq current vortex during the summer months (Yamazaki and Maute, 2017).

Table 1. Variance fraction (in %) of the geomagnetic field X, Y and Z components.

The minimum, maximum and mean values of the variance fraction associated with the first three principal components (PC1-PC3) and the cumulative variance fraction (Σ) for the first three PCs. Bold marks PCs that are essential for Sq extraction.

	X component			Y component			Z component		
	min	mean	max	min	mean	max	min	mean	max
PC1	**28.8**	**49.5**	**78.2**	**58.1**	**82.7**	**94.0**	**62.1**	**85.0**	**94.9**
PC2	**9.5**	**21.1**	**36.9**	1.7	6.5	22.0	1.9	6.2	17.9
PC3	**4.2**	**10.9**	**20.7**	1.1	3.5	8.5	0.8	3.1	10.9
Σ PC1-PC3	67.2	81.6	93.8	82.5	92.7	98.1	83.6	94.3	98.0

On the decadal timescale, VF of mode 1 anti-correlates with geomagnetic activity, whereas VFs for mode 2 and mode 3 correlate with geomagnetic activity level (see Tab. 2). This is expected since PC1s for the Y

and Z components are associated with Sq, while, consequently, PC2 and PC3 contain variations related to disturbances (e.g., SD and Dst): during years with higher geomagnetic activity the contribution of the disturbance-type variations to the total variability of the Y and Z components increases resulting in higher VF values.

Table 2
Correlation between VF and the solar and geomagnetic activity.

	X component			**Y component**			**Z component**		
	min	mean	max	min	mean	max	min	mean	max
PC1	**28.8**	**49.5**	**78.2**	**58.1**	**82.7**	**94.0**	**62.1**	**85.0**	**94.9**
PC2	**9.5**	**21.1**	**36.9**	1.7	6.5	22.0	1.9	6.2	17.9
PC3	**4.2**	**10.9**	**20.7**	1.1	3.5	8.5	0.8	3.1	10.9
Σ PC1-PC3	67.2	81.6	93.8	82.5	92.7	98.1	83.6	94.3	98.0

The correlation coefficients are calculated between the mean VF associated with a PC for the Y, Z and X components for a certain year, and corresponding mean values of the solar and geomagnetic indices. Only $|r| \geq 0.3$ are shown, with *p values* in parentheses (only *p values* ≤ 0.2 are shown). Statistically significant correlation coefficients (p values ≤ 0.05) are in bold.

These results agree with previous findings of Golovkov et al. (1978, 1989), Golovkov and Zvereva (1998, 2000) and De Michelis et al. (2010) for different epochs and latitudinal zones.

5 Performance Of Pca As A Tool To Extract Sq For The X Component

5.1 PCA applied to the X component

Figure 3 shows examples of PC1, PC2 and PC3 together with Sq_{IQD} for the X component. All PC1, PC2 and PC3 series as well as the Sq series can be found at Morozova et al. (2021b). There are two main types of the shape of the Sq X variations obtained from the COI data:

- Shape A: the curves with a minimum (or maximum) near the local noon and secondary (with a lower amplitude) maximum (or minimum, respectively) in the early morning or late afternoon (see Fig. 3a).

- Shape B: the curves with two minima and two maxima of comparable amplitudes (see Fig. 3b-c).

According to Amory-Mazaudier (1994 and 2009), and Anad et al. (2016), these two types of the shapes of the Sq X can be interpreted, e.g., as caused by an Sq current vortex with a focus located to the south (or to the north, respectively) of the COI location - shape A, or very close to the latitude of COI (40ºN) - shape B.

5.2 Classification of X component's PCs using correlation analysis

The comparison of PC1-PC3 obtained for the X component with corresponding Sq_{IQD} using the correlation analysis shows that, contrary to the Y and Z components, no PC is always classified as Sq. Figures 4-6 show the classification of PCs for the X component based on the correlation analysis using single and combined classification.

Single classification (Fig. 4): for the individual years' series PC1s and PC2s were classified as Sq at about the same rate (59 and 52 series, respectively, or 40-45% each) while PC3s are classified as Sq about three times less often (18 series or 14%). Only in 3 cases (2%) none of the first three PCs was classified as Sq. On the contrary, for the *"all years"* series (see Fig. 4, last columns) in 6 cases (50%) PC2s were classified as Sq and in 3 cases each either PC1s or PC3s (25% each) were classified as Sq.

Thus, for the single classification, the probabilities of PC1 or PC2 to be classified as Sq_{PCA} (or the probabilities of Sq-type variation to be filtered to the 1st or 2nd mode) are approximately equal and about three times higher than the probability of PC3 to be classified as Sq.

Combined classification (Figs. 5-6): for the individual years' series PC1s and PC3s were classified as Sq at the same rate (8 and 6 series, respectively, or 5-6%) while PC2s are classified as Sq about three times more often (15 series or 12%). The combinations of PCs were classified as Sq in 43 cases for PC1+PC2 (33%), in 25 cases for PC1+PC3 (19%) and 32 cases for PC2+PC3 (24%). Only in 2 cases (~1.5%) none of the first three PCs or their combination was classified as Sq. For the *"all years"* series (see Figs. 5-6, last columns) in 7 cases (58%) PC2+PC3 were classified as Sq, in 4 cases (33%) PC1+PC3 were classified as Sq, in 1 case (8%) PC2 was classified as Sq.

Thus, for the combined classification the most probable scenarios to extract Sq-type variations are (in the declining order) the combination of PC1+PC2, PC2+PC3 and PC1+PC3.

The results of both kinds of classification for the X component are in general agreement with previous results obtained for the European region (De Michelis et al., 2010): Sq_{PCA} tends to be more frequently associated with PC2 than with other components.

The advantage of the combined classification is that the higher values of *r* were obtained for sums of PCs compared to *r* for the individual PCs. In many cases the increase of the *r* values is small however in some other cases the use of a sum of PCs allows to increase the *r* value from 0.6-0.68 to 0.83-0.91 as, for example, are the case of June *all years* series, June 2009, July 2017, April 2015, or December *all years* series.

As follows from Tab. 1, the mean variance fractions for PC1-PC3 for the X component are ~50%, ~21% and ~11%, respectfully. The mean VF varies throughout the year: for PC1 it is higher in winter, and VFs of PC2 and PC3 are higher in summer. On the decadal time scale, see Tab. 2, VF of PC1 (PC2) correlates (anti-correlates) with variations of the geomagnetic activity through the 11-year cycle.

As one can see from Figs. 4-6, there is no clear seasonal or decadal pattern in the classification of PC1-PC3 for the X component as the Sq variation. We compared the number of months per year with PC1, PC2 or PC3 classified as Sq (single classification) with the annual mean values of the solar and geomagnetic activity indices. For the combined classification we made a similar comparison for the number of months per year with PC1+PC2, PC1+PC3 or PC2+PC3 classified as Sq (the number of single PCs classified as Sq using the combined classification is too low for a statistically significant analysis). The obtained correlation coefficients (Tab. 3) are low and statistically insignificant (*p values* > 0.2), however, we may conclude that, in general, the increase of the geomagnetic activity results in a more often classification of PC2 or PC1+PC3 as Sq variation; the increase of the solar activity results in a more often classification of PC1 or PC1+PC3 as Sq. We can interpret this as follows: for geomagnetically quiet epochs the Sq variation is, in most cases, the dominant variation for the X component and has a high probability to be filtered by PCA to the mode 1, while for the geomagnetically disturbed epochs the disturbance-type variations (like SD and Dst) became dominant and will be associated with PC1 while Sq will be rather filtered to the mode 2 or even to the mode 3. Similar behavior was shown by Golovkov et al. (1978, 1989) and Golovkov and Zvereva (1998, 2000) for data obtained at other latitudinal zones and for other decades. On the other hand, the increase of the solar activity results in a more intense flux of the solar UV radiation and, consequently, in higher ionization of the ionosphere, stronger Sq vortex and higher amplitude of the Sq geomagnetic variation. Unfortunately, the found dependence cannot be used to automatically define which PC is classified as Sq.

Table 3
Number of months with PCs classified as Sq vs mean values of the solar/geomagnetic indices.

		Geomagnetic indices				Solar indices	
		AE	ap	Kp	Dst	R	F10.7
Y component	PC1	-0.71 (0.15)	-0.78 (0.06)	-0.74 (0.09)			
	PC2	0.57	0.66 (0.13)	0.61 (0.19)			
	PC3	**0.81 (<0.01)**	**0.81 (0.01)**	**0.75 (0.03)**	-0.44		
Z component	PC1	-0.50	-0.56 (0.2)	-0.50		0.43	0.44
	PC2	0.64 (0.09)	**0.69 (0.05)**	0.63 (0.09)			
	PC3					**-0.54 (0.04)**	**-0.59 (0.02)**
X component	PC1					0.46 (0.17)	**0.54 (0.05)**
	PC2	-0.41 (0.12)	**-0.49 (0.04)**	-0.43 (0.13)	0.31		
	PC3						

Correlation coefficients between the number of months per year with PCs for X classified as Sq and mean annual values of the solar/geomagnetic indices. Only $|r| \geq 0.3$ are shown, with *p values* in parentheses (only *p values* ≤ 0.2 are shown). Statistically significant correlation coefficients (p values ≤ 0.05) are in bold.

Thus, for the X component, PCA cannot be used as a simple method to extract Sq variations without further classification of the modes, and a comparison to a reference series is needed to identify PC that represents Sq variation.

5.3 Adaptation of PCA for automatic extraction of Sq for the X component

As was shown in Section 5.2, for the X component is it impossible to automatically extract Sq variation using PCA. A certain reference series is needed to be compared with PCs to classify one of those PCs or a sum of PCs as Sq_{PCA}. In this work, we tested two types of reference series: (1) the mean Sq_{IQD} series obtained from geomagnetic field observations for a long-time-interval and (2) simulations of the ionospheric part of the geomagnetic field using geomagnetic field models.

Another important problem of the application of PCA to extract Sq-type variation from the series of the X component is that the high rate of the PCs' classification shown in Section 5.2 was obtained for a quite low threshold ($|r| \geq 0.45$). As one can see from Figs. 4-6, higher values of the threshold would significantly decrease the number of the identified PCs. On the other hand, the visual analysis of the corresponding PCs and Sq curves show that in some cases of the low *r* values the compared series show

quite similar variations and the low values of *r* are related to local compressions and stretches of one of the series relatively to another. Thus, we need a different metric as a base for the classification. We compared the performance of the Pearson correlation coefficient *r* and the *dtw* distance as a metric of the similarity of the studied series.

5.3.1 Mean Sq_{IQD} as a reference series

Sq_{IQD} series obtained for the same geomagnetic station or observatory seem to be a good choice for a reference series because they automatically incorporate features of the Sq variation associated with a particular location (shape of the daily curve, characteristic seasonal variations etc.). However, as was shown in Section 5.2, the Sq_{IQD} series obtained for an individual month and individual year cannot be used as reliable reference series. Firstly, the automatic usage of PCA implies that a reference series already exists. Secondly, Sq_{IQD} calculated for a particular month and year is strongly affected by the level of geomagnetic activity of those 5 IQDs that were used to calculate it. Thirdly, the position and the shape of the Sq current vortex in the ionosphere depends on the conditions in the upper atmosphere (wind strength, amplitude of waves and tides etc.). Thus, individual features of the vortex during the selected 5 IQDs are preserved in the Sq_{IQD} of the individual months. This can be of great importance for an analysis of the data obtained at observatories as COI when the position of the station to the north or the south to the Sq current vortex focus during selected days affects the Sq_{IQD} variation's curve dramatically. On the other hand, averaging the Sq_{IQD} variation series obtained for a certain month but for several years may reduce the effect of individual features caused by the varying geomagnetic and atmospheric conditions. Therefore, we tested the $Sq_{IQD\ allY}$ series, which were calculated for a particular month using data for all years from 2007 to 2017, as one of the reference series for the PCs' classification.

Overall, for most of the studied series (months from January to December, years from 2007 to 2017) there is a strong correlation between Sq_{IQD} and $Sq_{IQD\ allY}$, however, for some months (mostly autumn-winter months with weak Sq current vortex) there is a large variability in the Sq_{IQD} shape resulting in a lower correlation between two types of Sq_{IQD} (individual correlation coefficients can be found in [Additional file 4, Fig. S4.1, top]). The detailed analysis of the Sq_{IQD} and $Sq_{IQD\ allY}$ series shows that there are (1) cases of the low correlation which are caused simply by shifts of maxima/minima position, and (2) cases of (relatively) high correlation that result from the similarity of the general trend but not of individual features of the compared curves. To test if the DTW analysis can perform better in these situations we calculated the *dtw* values for each of the corresponding pairs of the Sq_{IQD} and $Sq_{IQD\ allY}$ series [Additional file 4, Fig. S4.1, bottom]. In general, it seems that the DTW analysis gives a more realistic estimate of the similarity between the Sq_{IQD} and $Sq_{IQD\ allY}$ series. Some examples of the DTW matching can be found in [Additional file 4, Figs. S4.2-S4.3]: Fig. S4.2 gives examples of the cases when (relatively) high *r* values are obtained for series with similar general trends but different local features – corresponding *dtw* are high which means bad matching between the curves; and Fig. S4.3 gives

examples of the cases when (relatively) low *r* values are obtained for series with similar features shifted locally – corresponding *dtw* are low which means good matching between the curves.

We used the $Sq_{IQD\ allY}$ series as reference series to classify PCs based both on the *r* and *dtw* metrics and using the combined classification option. The results (similar to Figs. 5-6) can be found in [Additional file 5, Figs. S5.1-S5.2 for *r* and Figs. S5.3-S5.4 for *dtw*]. Columns 1 and 4 of Tab. 4 show how many different PCs or their sums were classified as Sq_{PCA} using *r* and *dtw*, respectively.

Table 4
PCs of X or their sums classified as Sq.

		Geomagnetic indices				Solar indices	
		AE	ap	Kp	Dst	R	F10.7
Single classification	PC1	-0.48	-0.53 (0.18)	-0.47		0.32	0.34
	PC2	0.34	0.39	0.38			
Combined classification	PC1+PC2				0.4	-0.38	-0.33
	PC1+PC3				-0.38	0.53	0.57

Number (out of 144) of PCs or their sums classified as Sq using different reference series ($Sq_{IQD\ allY}$, CM5 and DIFI3) and different metrics (*r* and *dtw*).

5.3.2 Ionospheric field models as reference series

As mentioned in Section 3.2, we used two models to simulate the ionospheric part of the geomagnetic field: CM5 and DIFI3. These series were used as reference series for the PCs classification using both *r* and *dtw* metrics. The classification results (similar to Figs. 5-6) can be found in [Additional file 6, Figs. S6.1-S6.2 for *r* and Figs. S6.3-S6.4 for *dtw*] for CM5 and in [Additional file 7, Figs. S7.1-S7.2 for *r* and Figs. S7.3-S7.4 for *dtw*] for DIFI3. Table 4 (columns 2-3 and 5-6) shows numbers of different PCs or their sums that were classified as Sq_{PCA} using different reference series and different metrics.

5.4 Conclusions on the best reference series and best classification metrics

As one can see from Table 4, *dtw* allows classifying more series than *r*. Most of the series that were identified as Sq_{PCA} are sums of PCs: the sum PC1+PC2 is most often classified as Sq_{PCA} using all studied reference series and both metrics; it is followed by the sums PC2+PC3 and PC1+PC3 which are more or less equally often classified as Sq_{PCA}.

Even so, the differences between the performance of the analyzed reference series and metrics are small, we recommend the DIFI3 model as a reference series and the *dtw* as a metric to be used to identify PCs that correspond to the Sq-type variations of the X component of the geomagnetic field.

5.5 Comparison of different Sq series for the X component

As the final step, we compared the Sq-type variations extracted from the data using the IQD and PCA approaches, and the ionospheric field forecasted by the CM5 and DIFI3 models. The mean and median correlation coefficients between the Sq_{PCA} series (identified using combined classification with DIFI3 as a reference series and *dtw* as a metric) and the reference series (Sq_{IQD}, $Sq_{IQD\ allY}$, Sq_{CM5} and Sq_{DIFI3}) are $r_{mean} \sim 0.75$ and $r_{median} \sim 0.65$ (the individual correlation coefficients can be found in [Additional file 8]). Figure 7 shows two examples of the comparisons for Sq_{PCA} and the reference series. These plots also allow comparing Sq_{PCA} variations obtained for a certain month using the data only for a certain year (black lines) and for the *"all years"* series (grey lines). It seems that for months near equinoxes and solstices (February-March, May-June, August-October, December) it is better to use only data for the studied year to obtain a Sq_{PCA}, whereas for other months it is better to use data for this month but for several years of observations (11 in our case), however, this conclusion still needs to be confirmed on longer time series or data from other locations.

6 Conclusions

In this work, we analyzed the performance of the principal component analysis (PCA) as a tool to extract Sq variation from the geomagnetic field observations (X, Y and Z components) made at a mid-latitudinal station (Coimbra Magnetic Observatory, Portugal). The studied time interval is from January 2007 to December 2017; the time resolution is 1h. The data were analyzed individually for all 12 months. The geomagnetic field components were analyzed separately.

The PCA modes were compared to Sq variation obtained for the same month using the standard approach based on the calculation of the mean daily variations using 5 international quiet days (IQD), Sq_{IQD}, using both the correlation and the dynamic time warping (DTW) analyses. Only the first three PCA modes were analyzed. As reference series, the ionospheric field modelled using the CM5 and DIFI3 models were also used.

Based on correlation and DTW analyses some PCs were classified as Sq_{PCA}. Two approaches were tested: only one PC can be classified as Sq_{PCA} (single classification) or also a weighted sum of PCs can be classified as Sq_{PCA} (combined classification).

The number of the PCs classified as Sq and their order were analyzed in relation to the component, season (mean seasonal variations through a year) and year (mean decadal variations during the 11-year solar/geomagnetic activity cycle).

In this study, we assessed only the ability of PCA to obtain daily variations that are more or less similar to ones obtained from the measurements or predicted by models. No analysis of the shapes of the Sq variations themselves or the dependence of those shapes on the geomagnetic activity level and/or position of the Sq current vortex was made.

It was found that for the Y and Z components the Sq variation is always filtered to the first PCA mode (PC1). Thus, PCA can be used to extract Sq variations from the observations of the Y and Z geomagnetic field components without any additional procedures. For the studied time interval and for the mid-latitudinal geomagnetic data we found no limitations or constraints to the usage of PCA as a tool to extract Sq variations from the Y and Z components' series. There are no significant differences in PC1s obtained for a certain month for an individual year and several years (11 years in our case), thus the input data set with the length of ~1 month (not necessary coinciding with a calendar month) will be sufficient to extract reliable Sq variation from the series of the Y and Z component.

Application of PCA to the series of Y and Z allowed us to estimate the fraction of the total variance of the Y and Z series that can be associated with Sq variation: ~83% on average. The variance fraction of PC1 and, consequently, of Sq, increases in summer, the season with higher insolation and higher intensity of the ionospheric currents producing the Sq variation. Also, as expected, for the years with higher geomagnetic activity levels the variance fraction of the first mode decreases and the variance fractions of the second and third modes, which most probably contain disturbance-type variations, increase.

The classification of PCs obtained for the X component is much more complicated, probably, due to the higher contribution of the geomagnetic disturbances into the variability of the X component at the middle latitudes. First, all three first PCs can be classified as Sq. No patterns in the classification rate of different PCs related to the season or the level of the solar/geomagnetic activity were found. Thus, PCA can be used to extract Sq variation from the observations of the X component, but further analysis (for example, a comparison to a set of reference curves either obtained from the data analysis or generated using models) is always needed to classify PCs of the X component.

Two types of reference series were tested: the Sq_{IQD} series obtained for each month using all years of observations (11 years), and the ionospheric magnetic field modelled using the CM5 and DIFI3 models. The reference series were compared to PCs using two metrics: the correlation coefficient *r* and the DTW distance (*dtw*). In general, all reference series and both metrics performed well, however only the combination of the DIFI3 model as a reference series and the *dtw* metric allowed us to identify Sq_{PCA} for all analyzed series.

Therefore, PCA can be used to extract Sq variation from the observations of the X component if followed by a classification procedure using a reference series (preferably DIFI3 ionospheric field). Both the correlation and the DTW analyses can be used for classification, but DTW seems to perform better.

Another advantage of the usage of reference series is that it allows solving a “sign ambiguity problem” for PCs that are obtained using SVD (see Section 3.3.1) There is no general way to solve the sign ambiguity, and comparison to a reference series can be an easy way to do so. This may apply not only to the X but also to the Y and Z series.

Finally, we list the main advantages and disadvantages of the usage of the PCA method to extract Sq-type variation from the observations of the geomagnetic field components that we found:

PCA advantages:

– With PCA there is no need to estimate the (relative) level of geomagnetic activity of different days of an analyzed month (or another time interval of a comparable length) to find geomagnetically quiet days (e.g., international or local quiet days). All available days of an analyzed time interval can be used.

– It is well known that Sq_{IQD} can be contaminated by the disturbance field (Yamazaki and Maute, 2017) since not all IQDs of a certain month could be quiet in the absolute sense. However, since PCA is applied to the month-long time interval, this method may allow extracting the Sq variation that has less contribution from the disturbance field. Thus, PCA allows to minimize the effect of the geomagnetic activity during individual days and to obtain the Sq variation that is more typical for the studied month.

– The shape of the Sq variation observed at a certain location depends on the position of the geomagnetic observatory relative to the focus of the Sq current vortex. Thus, under certain circumstances, Sq_{IQD} could reflect not the general conditions in the ionosphere and the upper atmosphere during a certain month but some individual features (position of the focus and the shape) of the vortex during IQDs. On the other hand, while PCA is applied to the month-long time interval, this method may allow to minimize the effect of the individual days and to obtain a more “climatological” Sq variation.

– PCA allows the estimation of the variance fraction associated with a mode that is classified as Sq.

– The EOF functions available for each of the PCs for each day of the analyzed time interval permit reconstructing the amplitudes of the Sq variation for each day individually allowing the assessment of its day-to-day variability.

PCA disadvantage:

– The automatic classification of PCs is not always straightforward. For the Y and Z components, the Sq variations seem to be always filtered to PC1, however for the X component an additional manual or automatic classification is needed (e.g., by comparing PCs to a set of reference curves).

Abbreviations

Ap, AE, Kp and Dst indices of geomagnetic activity level

COI Coimbra magnetic Observatory

CM5 the comprehensive model 5

CIRES Cooperative Institute for Research in Environmental Sciences at the University of Colorado Boulder

DIFI3 The Dedicated Ionospheric Field Inversion model 3

DTW the dynamic time warping

EOFs empirical orthogonal functions

EEJ the equatorial electrojet

ESA European Space Agency

F10.7 index reflecting variations of the solar UV flux

GFZ German Research Centre for Geosciences at the Helmholtz Centre in Potsdam

IQD international quiet day

IAGA International Association of Geomagnetism and Aeronomy

NOC the natural orthogonal component method

PCA principal component analysis

PC(s) principal component(s)

PC1 1st principal component

PCn principal component of the n order

R the sunspot number series reflecting variations of the solar UV flux

r correlation coefficient

Sq Solar quiet variation

SD Solar disturbed variation

Sq_{PCA} Solar quiet variations obtained using PCA

Sq_{IQD} Solar quiet variations obtained using IQD

Sq_{CM5} Solar quiet variations obtained using CM5

Sq_{DIFI3} Solar quiet variations obtained using DIFI3

SVD The singular value decomposition

SCARF Satellite Constellation Application and Research Facility (SWARM product)

VF variance fraction

Declarations

Ethics approval and consent to participate

Not applicable.

Consent for publication

Not applicable.

Availability of data and materials

The COI 1h data for all geomagnetic components can be downloaded from the World Data Centre for Geomagnetism using the Geomagnetism Data Portal at http://www.wdc.bgs.ac.uk/dataportal/ (station name: “Coimbra”, IAGA code: “COI”).

The Sq_{IQD} and PCs analyzed in the paper can be downloaded at *Mendeley Data*, doi: 10.17632/jcmdrm5f5x.1, http://dx.doi.org/10.17632/jcmdrm5f5x.1.

All indices of the solar and geomagnetic activity used in this work can be downloaded from the OMNI database at https://omniweb.gsfc.nasa.gov/form/dx1.html.

CM5 model is available at https://ccmc.gsfc.nasa.gov/models/modelinfo.php?model=CM5.

The DIFI3 model is available at http://geomag.colorado.edu/difi-calculator.

A package for R to calculate *dtw* with different algorithms that were used in this study was developed by Giorgino (2009) and can be downloaded from https://cran.r-project.org/web/packages/dtw/index.html.

Competing interests

AM and RR have no financial and non-financial competing interests.

Funding

CITEUC is funded by the National Funds through FCT (Foundation for Science and Technology) projects UID/00611/2020 and UIDP/00611/2020.

IA is supported by FCT through the research grants UIDB/04434/2020 and UIDP/04434/2020.

This study is a contribution to the MAG-GIC project (PTDC/CTA-GEO/31744/2017), and RR is funded through this project.

Authors' contributions

Anna Morozova: Conceptualization, Formal analysis, Methodology, Supervision, Validation, Software, Investigation, Visualization, Writing - original draft.

Rania Rebbah: Software, Investigation, Data processing, Visualization, Writing - review & editing.

Acknowledgements

AM is thankful to Dr. T. Giorgino for the development of the "dtw" R package (https://dynamictimewarping.github.io/, http://dtw.r-forge.r-project.org/)

References

1. Amory-Mazaudier, C (1994) On the electric current systems in the Earth's environment some historical aspects Part I: external part/ ionosphere/quiet variation, special issue on the IAGA meeting in Buenos Aires published in GEOACTA 21, 1-15.
2. Amory-Mazaudier, C August (2001) On the electric current systems in the Earth's environment some historical aspects. Part II: external part/ionosphere/disturbed variation from the IAGA Assembly in Hanoï Vietnam..
3. Amory-Mazaudier, C (2009) Electric current systems in the earth’s environment J. Space Res., 8, pp.178-255, Niger.
4. Anad, F., Amory-Mazaudier, C., Hamoudi, M., Bourouis, S., Abtout, A. and Yizengaw, E(2016)Sq solar variation at Medea Observatory (Algeria), from 2008 to 2011. Advances in Space Research, 58(9), pp.1682-1695.doi: 10.1016/j.asr.2016.06.029
5. Bhardwaj, S.K. and Rao, P.S.September(2016)Longitudinal inequalities in Sq current system along 200-2100 E meridian. J. Ind. Geophys. Union, 20(5), pp.462-471.
6. Bhardwaj, S.K., Rao, P.S. and Veenadhari, B(2015)Abnormal quiet day variations in Indian region along 75 E meridian. Earth, Planets and Space, 67(1), pp.1-15.
7. Björnsson, H. and Venegas, S.A.(1997) A manual for EOF and SVD analyses of climatic data. *CCGCR Report*, *97*(1), pp.112-134.
8. Chapman, S. and Bartels, J., (1940) *Geomagnetism.* Oxford University Press, Oxford.
9. Chen, G.X., Xu, W.Y., Du, A.M., Wu, Y.Y., Chen, B. and Liu, X.C. (2007): Statistical characteristics of the day-to-day variability in the geomagnetic Sq field. Journal of Geophysical Research: Space Physics, 112(A6), doi:10.1029/2006JA012059.
10. Chulliat, A., Vigneron, P., Thébault, E., Sirol, O., & Hulot, G. (2013)Swarm SCARF dedicated ionospheric field inversion chain. *Earth, Planets and Space*, *65*(11), 1271–1283. doi:10.5047/eps.2013.08.006
11. Chulliat, A., Vigneron, P., & Hulot, G. (2016)First results from the Swarm Dedicated Ionospheric Field Inversion Chain Swarm Science Results after two years in Space 1. Geomagnetism. *Earth, Planets and Space*, *68*(1). doi:10.1186/s40623-016-0481-6
12. De Michelis, P., Tozzi, R. and Consolini, G. (2010)Principal components’ features of mid-latitude geomagnetic daily variation. Ann. Geophys, 28, pp.2213-2226, doi:10.5194/angeo-28-2213-2010.
13. De Michelis, P., Tozzi, R. and Meloni, A. (2009) On the terms of geomagnetic daily variation in Antarctica. Ann. Geophys, 27, pp.2483-2490.

14. Ebisuzaki, W. (1997) A method to estimate the statistical significance of a correlation when the data are serially correlated, J. Clim., 10 (9), 2147-2153.
15. Giorgino, T., (2009) Computing and visualizing dynamic time warping alignments in R: the dtw package. Journal of statistical Software, 31(1), pp.1-24, doi: 10.18637/jss.v031.i07.
16. Golovkov V.P., Zvereva T.I. (1998) Expansion of Geomagnetic Variations within a Year in Natural Orthogonal Components, Geomagn. Aeron., 38, 368-372
17. Golovkov, V. P., and T. I. Zvereva (2000), The space-time pattern of midlatitude geomagnetic variations, Geomagn. Aeron., 40, 84–92.
18. Golovkov, V. P., N. E. Papitashvili, Y. S. Tyupkin, and E. P. Kharin (1978), Separation of geomagnetic field variations into quiet and disturbed components by the method of natural orthogonal components, Geomagn. Aeron., 18, 342–344.
19. Golovkov, V. P., V. O. Papitashvili, and N. E. Papitashvili (1989), Automatic calculation of K indices using the method of natural orthogonal components, Geomagn. Aeron., 29, 514–517.
20. Haines, G.V. and Torta, J.M. (1994): Determination of equivalent current sources from spherical cap harmonic models of geomagnetic field variations. Geophysical Journal International, 118(3), pp.499-514.
21. Hannachi, A., Jolliffe, I.T. and Stephenson, D.B.(2007) Empirical orthogonal functions and related techniques in atmospheric science: A review. *International Journal of Climatology: A Journal of the Royal Meteorological Society*, *27*(9), pp.1119-1152.doi: **10.1002/joc.1499**.
22. Maslova, I., Kokoszka, P., Sojka, J. and Zhu, L. (2010): Estimation of Sq variation by means of multiresolution and principal component analyses. Journal of Atmospheric and Solar-Terrestrial Physics, 72, 7-8, 625-632.doi: 10.1016/j.jastp.2010.02.005.
23. Menvielle, M., (1981) About the scalings of K indicesfrom IAGA News, 20, p.110-111.
24. Morozova, A.L., Rebbah, R., and Ribeiro, P., (2021a). Datasets of the solar quiet (Sq) and solar disturbed (SD) variations of the geomagnetic field at the Coimbra Magnetic Observatory (COI) obtained by different methods, *Data in Brief*, v. 37C, 107174, doi:10.1016/j.dib.2021.107174.
25. [dataset] Morozova, A.L., Rebbah, R., and Ribeiro, P., (2021b). Datasets of the solar quiet (Sq) and solar disturbed (SD) variations of the geomagnetic field at a midlatitudinal station in Europe obtained by different methods, *Mendeley Data*, V1, doi: 10.17632/jcmdrm5f5x.1, http://dx.doi.org/10.17632/jcmdrm5f5x.1
26. Morozova, A.L., Ribeiro, P. and Pais, M.A., (2021c) Homogenization of the historical series from the Coimbra Magnetic Observatory, Portugal. *Earth System Science Data,* 13, 809–825, doi: 10.5194/essd-13-809-2021.
27. Morozova, A.L., Ribeiro, P. and Pais, M.A., (2014) Correction of artificial jumps in the historical geomagnetic measurements of Coimbra Observatory, Portugal. *Annales Geophysicae,* Vol. 32, No. 1, pp. 19-40, doi:10.5194/angeo-32-19-2014.
28. Piersanti, M., Alberti, T., Bemporad, A., Berrilli, F., Bruno, R., Capparelli, V., Carbone, V., Cesaroni, C., Consolini, G., Cristaldi, A. and Del Corpo, A. (2017): Comprehensive analysis of the geoeffective solar

event of 21 June 2015: Effects on the magnetosphere, plasmasphere, and ionosphere systems. Solar Physics, 292(11), p.169.doi:10.1007/978-94-024-1570-4_12.

29. Rangarajan, G.K. and Murty, A.V.S., (1980) Scaling K-indices without subjectivityFrom IAGA news, 19, 112-118.
30. Sabaka, T. J., Olsen, N., & Langel, R. A. (2002). A comprehensive model of the quiet-time, near-Earth magnetic field: Phase 3. *Geophysical Journal International*, *151*(1), 32–68. doi:10.1046/j.1365-246X.2002.01774.x
31. Sabaka, T.J., Tøffner-Clausen, L., Olsen, N. and Finlay, C.C., (2020) CM6: a comprehensive geomagnetic field model derived from both CHAMP and Swarm satellite observations. *Earth, Planets and Space*, *72*, pp.1-24.doi: 10.1186/s40623-020-01210-5.
32. Shlens, J., (2009) A Tutorial on Principal Component Analysis Center for Neural Science. *New York University New York City, NY*, pp.10003-660
33. Stening, R., Reztsova, T. and Minh, L.H. (2005): Day-to-day changes in the latitudes of the foci of the Sq current system and their relation to equatorial electrojet strength. Journal of Geophysical Research: Space Physics, 110(A10), A10308, doi:10.1029/2005JA011219.
34. Stening, R.J. (2008): The shape of the Sq current system. Annales Geophysicae (Vol. 26, No. 7, pp. 1767-1775).
35. Takeda, M. (1982). Three dimensional ionospheric currents and field aligned currents generated by asymmetric dynamo action in the ionosphere. Journal of Atmospheric and Terrestrial Physics, 44(2), 187–193. doi:10.1016/0021-9169(82)90122-2
36. Thébault, E., Vigneron, P., Langlais, B., & Hulot, G. (2016). A Swarm lithospheric magnetic field model to SH degree 80 Swarm Science Results after two years in Space 1. Geomagnetism. Earth, Planets and Space, 68(1). doi:10.1186/s40623-016-0510-5
37. Wu, Y.Y., Xu, W.Y., Chen, G.X., Chen, B. and Liu, X.C., (2007). The Evolution Characteristics of Geomagnetic Disturbances During Geomagnetic Storm. Chinese Journal of Geophysics, 50(1), pp.1-11.
38. Xu, W.Y. and Kamide, Y. (2004): Decomposition of daily geomagnetic variations by using method of natural orthogonal component. Journal of Geophysical Research: Space Physics, 109(A5).doi: **10.1029/2003JA010216**.
39. Yamazaki, Y. and Maute, A. (2017): Sq and EEJ—A review on the daily variation of the geomagnetic field caused by ionospheric dynamo currents. Space Science Reviews, 206(1-4), pp.299-405.doi: 10.1007/s11214-016-0282-z.

Figures

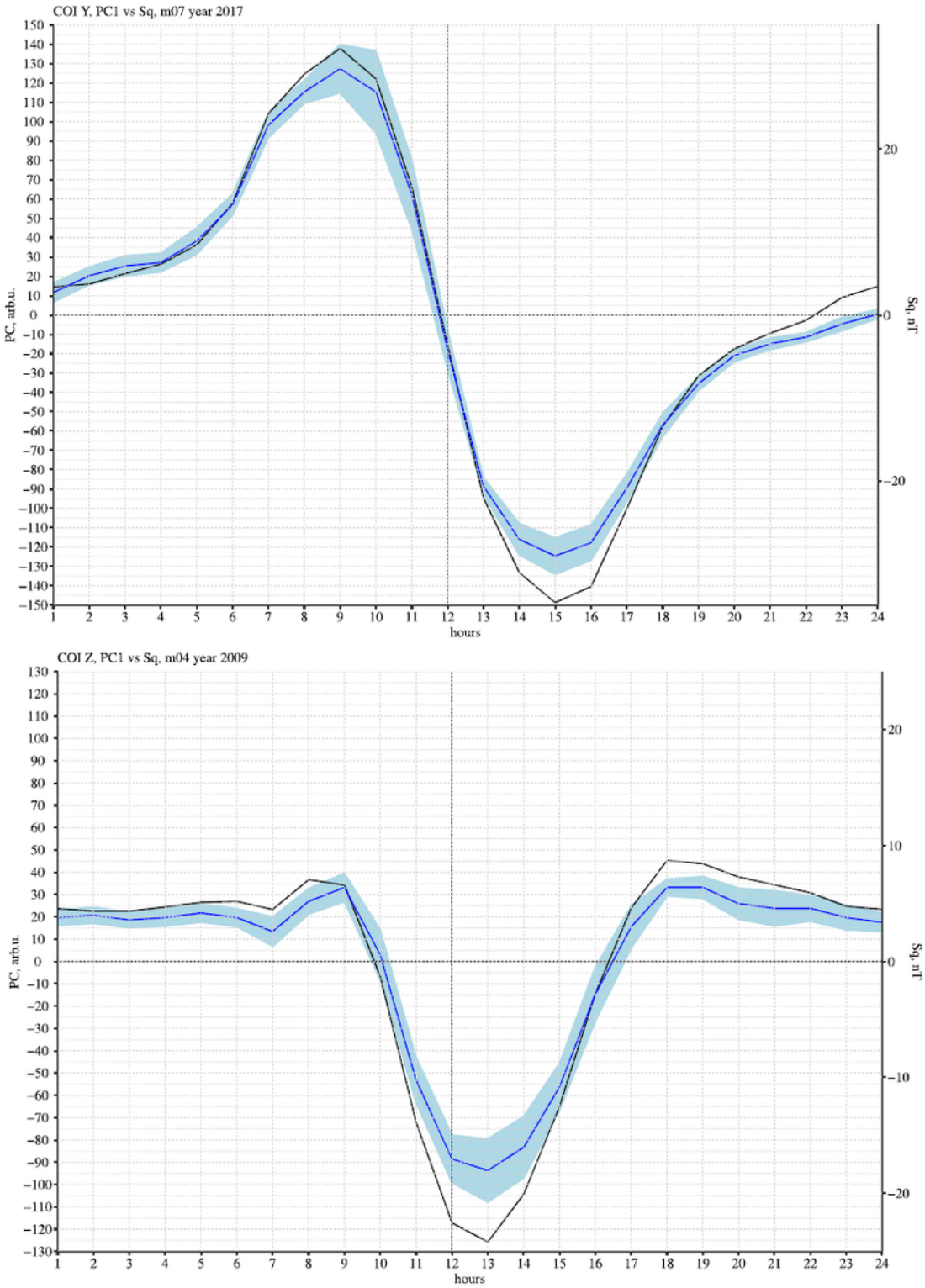

Figure 1

Examples of Sq_{IQD} and PC1 daily variations for Y and Z. Sq_{IQD} (blue lines, in nT) and PC1 (black lines, in a.u.) daily variations for the Y (top) and Z (bottom) components. Light blue bands show Sq_{IQD} ± SE values.

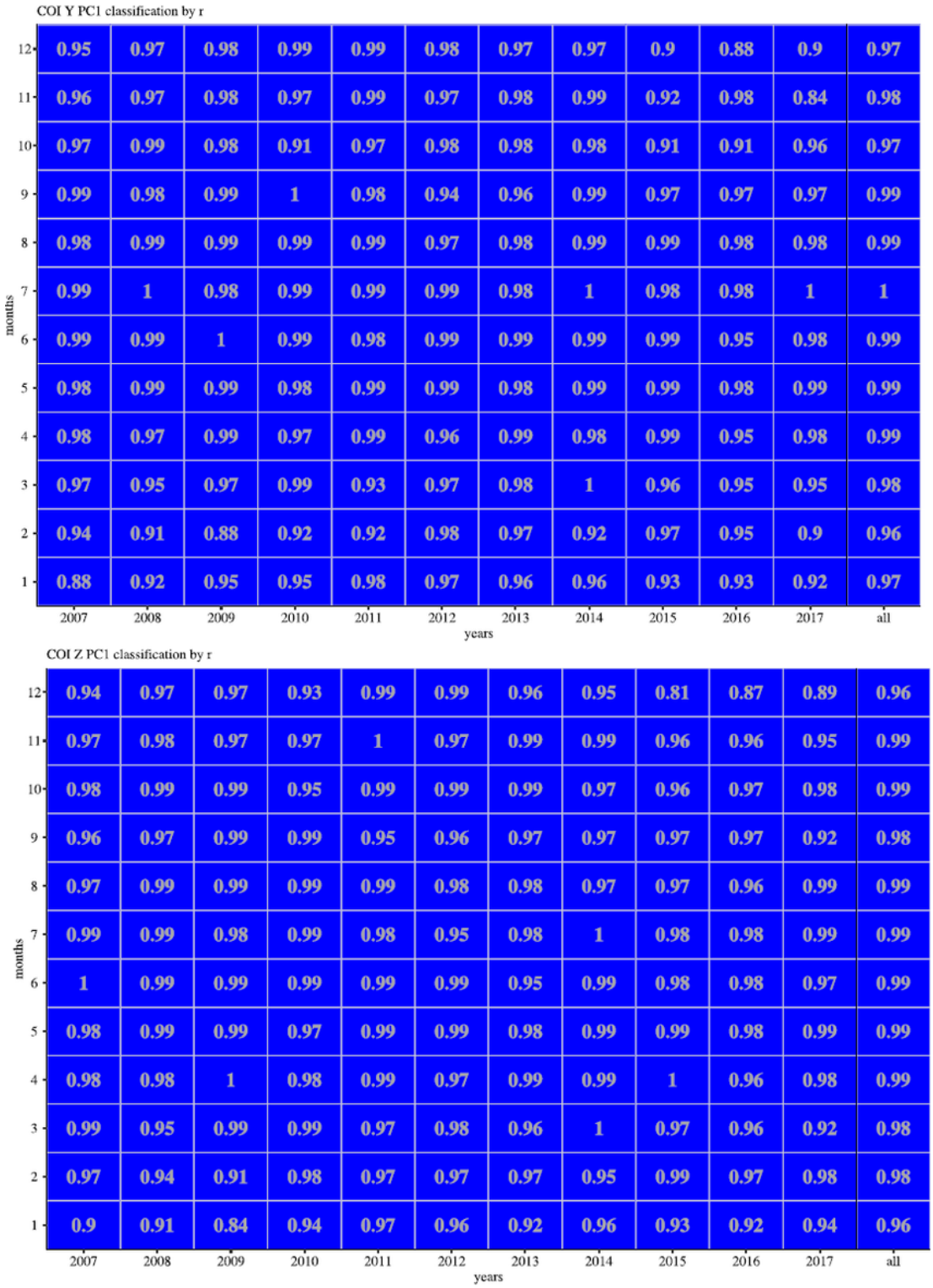

Figure 2

Correlation coefficients between the Sq_{IQD} and PC1 series for Y and Z. Numbers show correlation coefficients for the Y (top) and Z (bottom) components for different months (Y-axis) and different years (X-axis). Blue tiles mark the PCs classified as Sq (single classification using *r*).

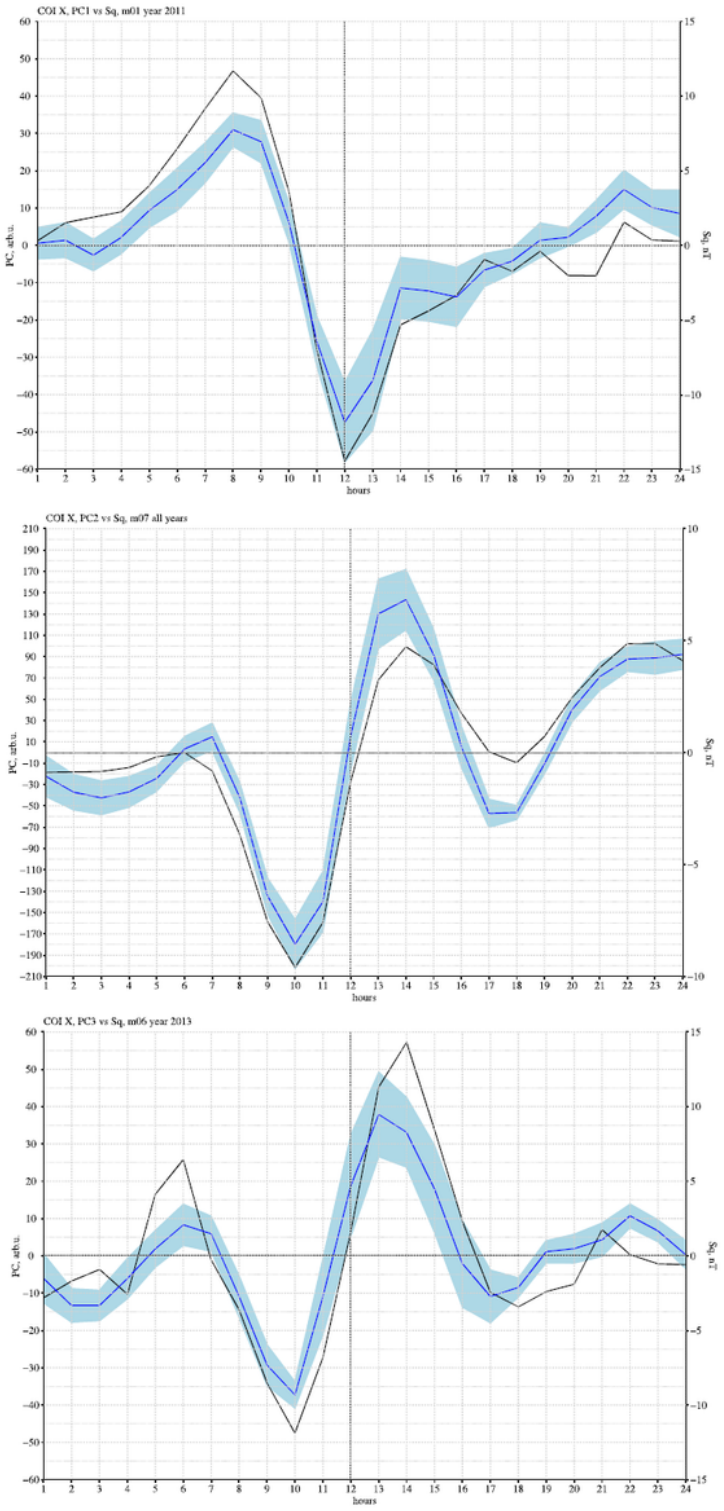

Figure 3

Examples of Sq_{IQD} and PC1 daily variations for X. Sq_{IQD} (blue lines, in nT) and PC1 (top), PC2 (middle) and PC3 (bottom) daily variations (black lines, in a.u.) for the X component. Light blue bands show Sq_{IQD} ± SE values.

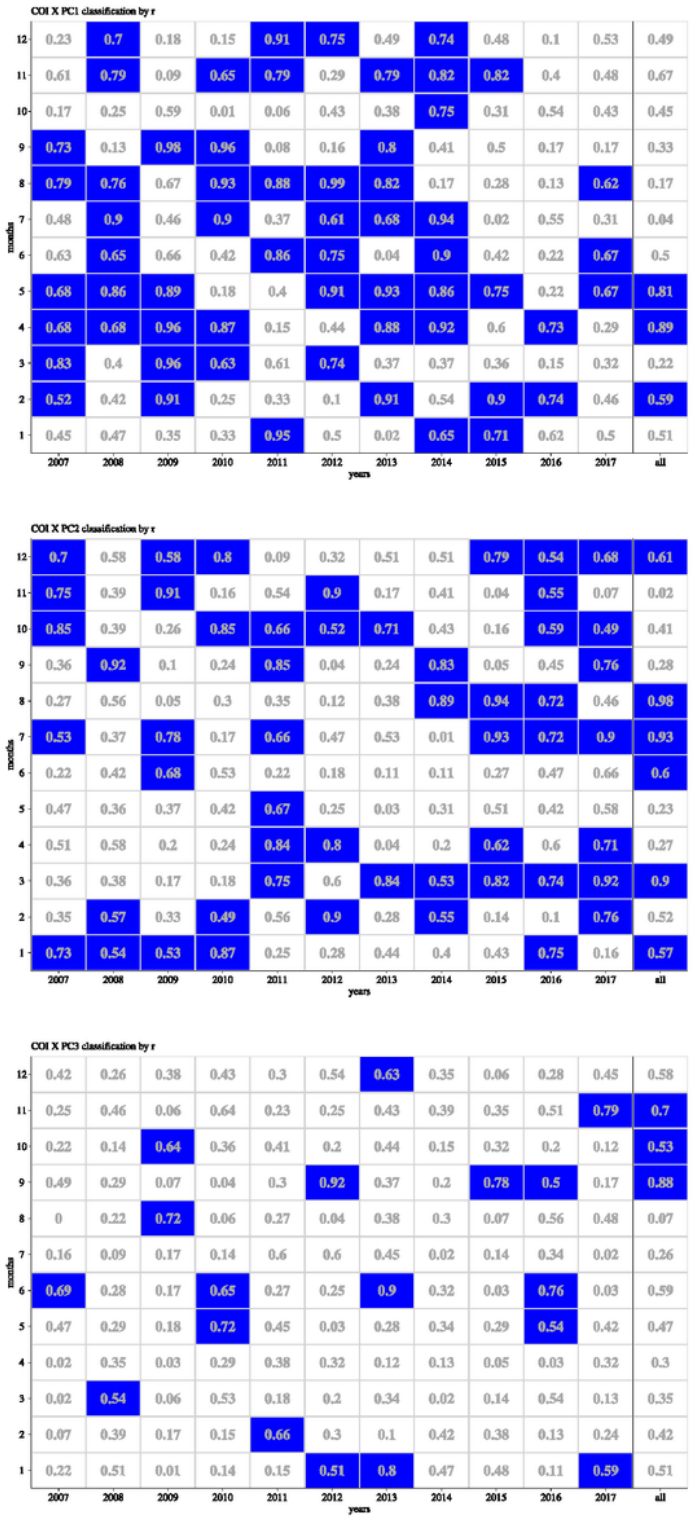

Figure 4

Correlation coefficients between the Sq_{IQD} and PCs for X (single classification). Correlation coefficients between the Sq_{IQD} and PC1 (top), PC2 (middle) and PC3 (bottom) series for the X component for different months (Y-axis) and different years (X-axis). Blue tiles mark PCs classified as Sq (single classification using *r*). Numbers show corresponding correlation coefficients.

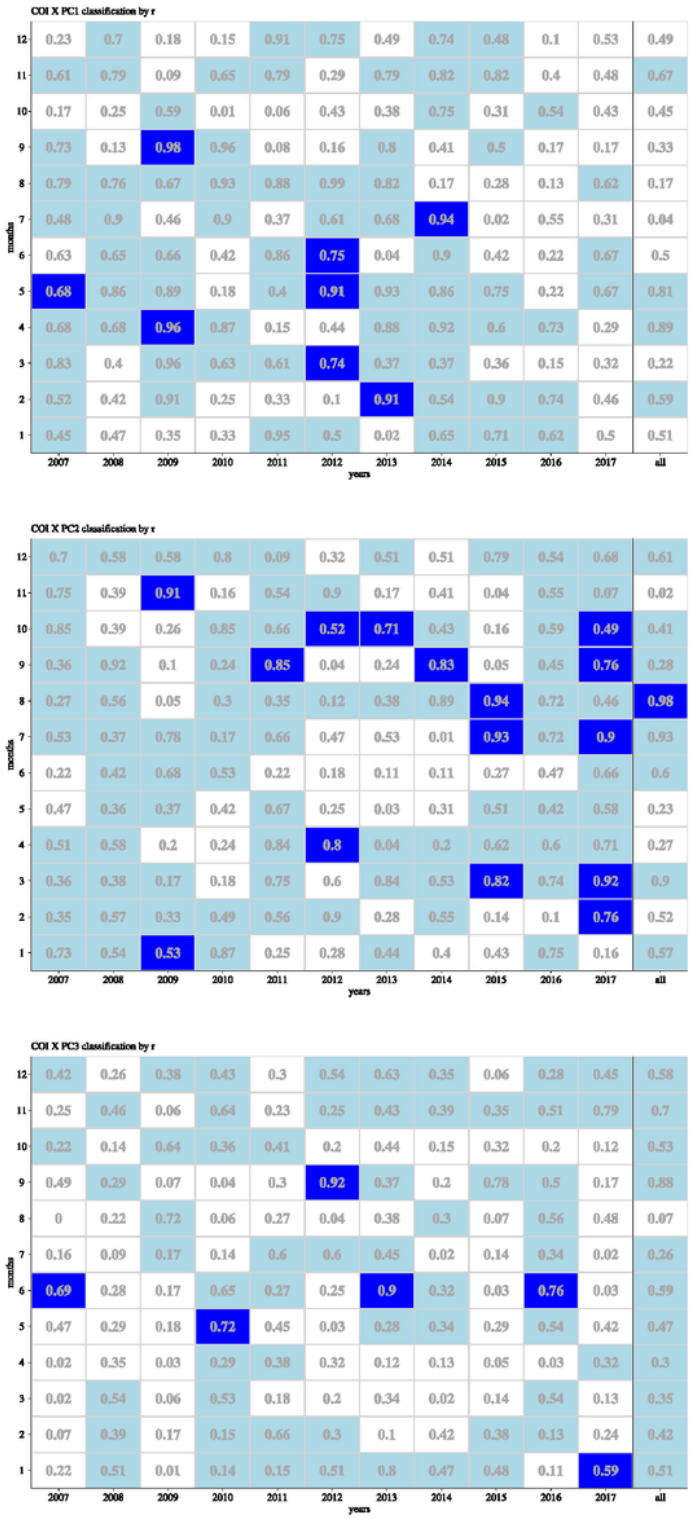

Figure 5

Correlation coefficients between the Sq_{IQD} and PCs for X (combined classification). Same as Figure 5 but with the combined classification allowed. Light blue tiles mark PCs classified as Sq in pairs with another PC (see Figure 6).

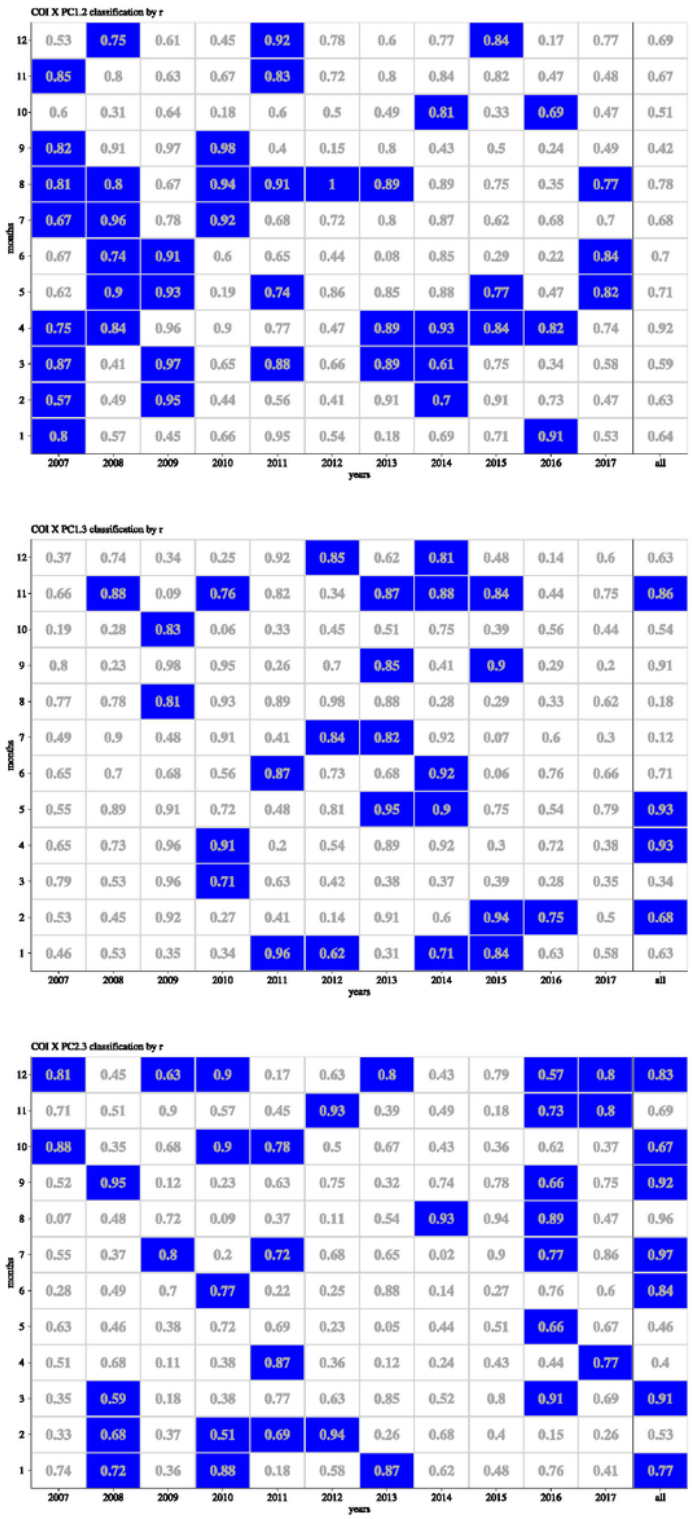

Figure 6

Correlation coefficients between the Sq_{IQD} and sums of PCs for X (combined classification). Same as Fig. 5 but for sums of PCs: top – PC1+PC2, middle – PC1+PC3, bottom – PC1+PC3.

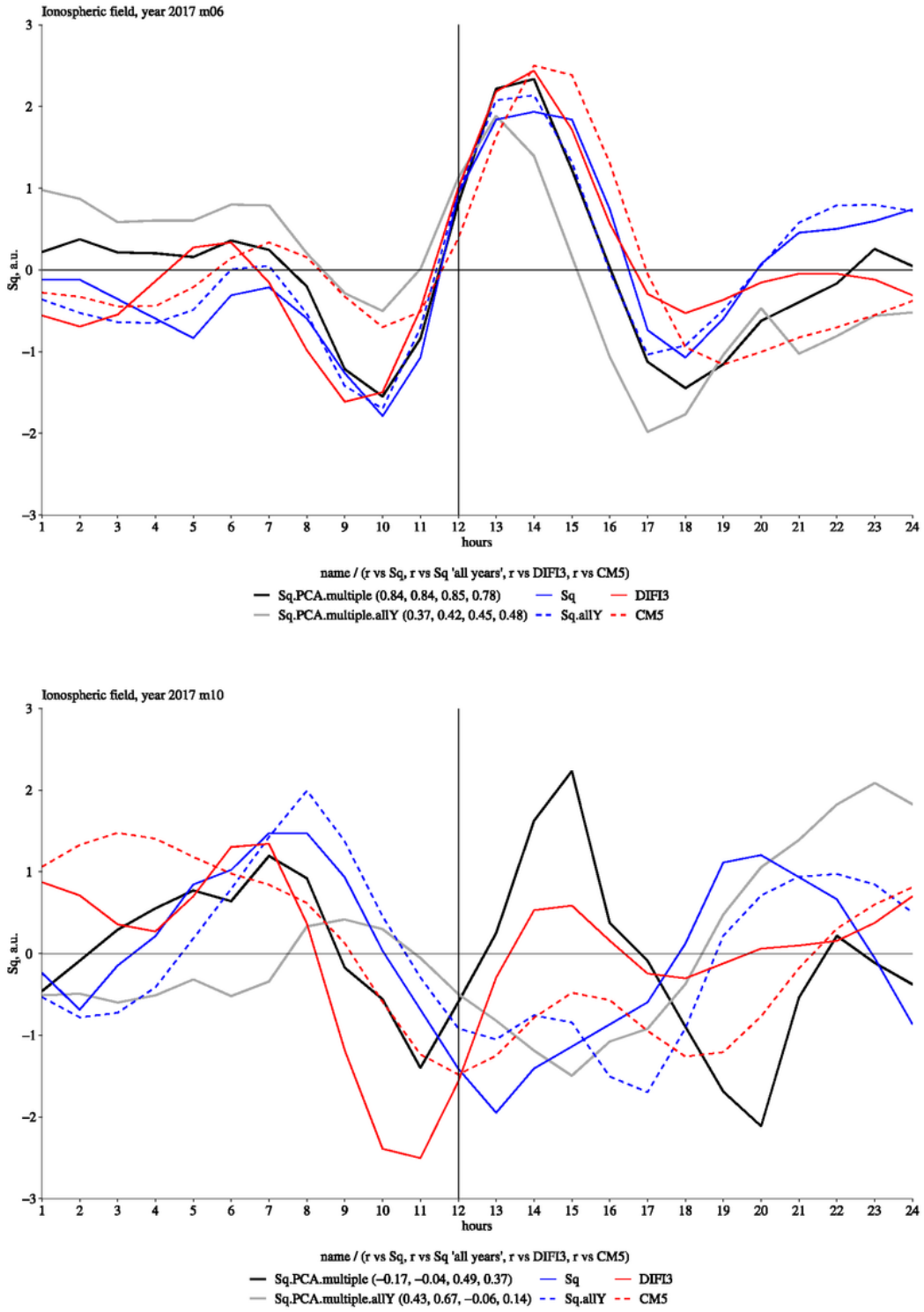

Figure 7

Examples of different types of Sq for the X component. Sq-type variations observed or predicted for June (top) and October (bottom) of 2017: Sq_{PCA} for June or October of 2017 – black lines; Sq_{PCA} for June or October of *all years* – grey lines; Sq_{IQD} for June or October of 2017 – blue solid lines, $Sq_{IQD\ allY}$ for June or October of *all years* – blue dashed lines; Sq_{DIFI3} for June or October – red solid line; Sq_{CM5} for June or

October – red solid line. Corresponding correlation coefficients between Sq_{PCA} and reference series are shown below the plots.

Supplementary Files

This is a list of supplementary files associated with this preprint. Click to download.

- GMFPCAAnalysisEPSAddFile1v1.pdf
- GMFPCAAnalysisEPSAddFile2v1.pdf
- GMFPCAAnalysisEPSAddFile3v1.pdf
- GMFPCAAnalysisEPSAddFile4v1.pdf
- GMFPCAAnalysisEPSAddFile5v1.pdf
- GMFPCAAnalysisEPSAddFile6v1.pdf
- GMFPCAAnalysisEPSAddFile7v1.pdf
- GMFPCAAnalysisEPSAddFile8v1.pdf
- GMFPCASChemev3aAM.png